IEEE/CSC & ESAS European Superconductivity News Forum (ESNF), No. 6, October 2008
(ASC Preprint 1MX05 conforming to IEEE Policy on Electronic Dissemination, Section 8.1.9)
The published version of this manuscript appeared in *IEEE Transactions on Applied Superconductivity* **19**, No. 3, Part 3, 3258 - 3261 (2009)

Enhanced vortex pinning in nanostructured YBCO/BZO coated conductors from chemical solution deposition

Alberto Pomar, Valentina Roxana Vlad, Anna Llordés, Anna Palau, Joffre Gutiérrez, Susagna Ricart, Teresa Puig, Xavier Obradors, Alexander Usoskin

***Abstract*—We present our latest results on the growth of chemical solution deposited $YBa_2Cu_3O_7$-$BaZrO_3$ nanocomposites on metallic substrates. All chemical ^{TFA}YBCO-BZO/^{MOD}CZO/^{ABAD}YSZ/SS tapes with J_c(77K,sf) = 1.7 MA/cm^2 have been achieved with smoother field dependence of J_c than that of standard ^{TFA}YBCO tapes. Angular resolved measurements show isotropic enhancement vortex pinning due to the presence of randomly oriented BZO nanoparticles in the YBCO matrix. Chemical routes are thus a promising way to efficiently increase vortex pinning in coated conductor and improve their capabilities for high field applications.**

***Index Terms*— Coated conductors, critical current density, nanocomposites, vortex pinning, nanostructured YBCO thin films.**

I. INTRODUCTION

THE quest for novel approaches to nanoengineer the microstructure of superconductors and thus to enhance vortex pinning in $YBa_2Cu_3O_7$ coated conductors has been a hot issue in these last years [1-6]. Among the different proposals, the growth of $YBa_2Cu_3O_7$-$BaZrO_3$ (YBCO-BZO) nanocomposites by chemical solution deposition combines the advantages of low-cost techniques together with astonishing performances in superconducting materials (for example, maximum pinning forces of 78 GN/m^3 at 65K with an effective anisotropy tending to unity) [4, 7, 8]. This remarkable pinning behavior is a consequence of the highly defective YBCO microstructure arising from the strain caused in the YBCO matrix by the random oriented $BaZrO_3$ nanoparticles [4, 8]. This random formation of nanoparticles seems to be easily obtained by chemical routes [4, 8, 9], although crystals orientation have also been reported [10]. This is indeed their major difference with the physical deposition techniques where, usually, coherent particles are obtained and vortex pinning enhancement is strongly anisotropic along the direction of the induced defects [5]. Moreover, as recently suggested, microstructure of the superconducting films and, therefore, vortex pinning, are strongly dependent on growth temperature and conditions [11]. For this reason, it is important to investigate the growth of chemical solution YBCO-BZO nanocomposite in different substrates and under different growth conditions in order to successfully transfer this technological approach to metallic tapes.

In this work we will present our latest results on the growth of YBCO-BZO nanocomposites made by the trifluoroacetates route on top of $(Ce,Zr)O_2$ (CZO) buffer layers. CZO layers were grown by metallorganic deposition (MOD) on YSZ single crystals and ^{ABAD}YSZ-stainless steel (SS) tapes. The pinning properties of the nanocomposite coated conductors are investigated by angular resolved transport measurements.

II. EXPERIMENTAL DETAILS

Chemical solution deposited epitaxial c-axis oriented YBCO/BZO nanocomposites were grown on metal organic deposited $(Ce,Zr)O_2$ buffered YSZ single crystals and ^{ABAD}YSZ stainless steel tapes. Films were prepared from anhydrous precursors solutions with stoichiometric quantities of Y, Ba and Cu trifluoroacetates (TFA) with the addition of Ba trifluoroacetate and Zr acetylacetonate. In this work the BZO molar content was fixed at 7%. A detailed description on solution preparation can be found in our previous work [4, 12]. After spinning on the substrate, samples were calcinated in a fast (<1.5h) pyrolysis process previously reported [13] where samples are heated in wet oxygen atmosphere up to 310ºC. After pyrolysis, films are grown during 150 min at high temperature (between 770ºC and 810ºC) in a wet, $P(H_2O)$=22mbar, nitrogen atmosphere with a partial oxygen pressure of 0.2 mbar. Superconducting phase is achieved after an oxygenation process performed at 450ºC in flowing oxygen gas. With the above growth conditions we have previously demonstrated that standard ^{TFA}YBCO films of 275 nm with self-field critical current densities as high as 5.2 MA/cm^2 can be obtained on chemical deposited $(Ce,Zr)O_2$ buffer layers on YSZ single crystals [14, 15]. When films are deposited on ABAD metallic tapes, buffered with ^{MOD}CZO layers, self-field values of critical current of ^{TFA}YBCO films were 1.8MA/cm^2 [15]. In all cases, the CZO layers were prepared from

Manuscript received 21 August 2008. This work was supported by Spanish Government national funds (MAT2005-02047, NAN2004-09133-C03-01, Consolider NANOSELECT CSD2007-00041), Generalitat de Catalunya (Pla de Recerca SGR-0029, XeRMAE) and European Union (HIPERCHEM and NESPA projects).

A.P. V.R.V., A.Ll., A.P. J.G., S.R., T.P. and X.O. are with Institut de Ciència de Materials de Barcelona, ICMAB-CSIC, Campus de la UAB, Bellaterra 08193 Spain (corresponding author e-mail: apomar@icmab.es).

A.U. is with the European High Temperature Superconductors GmbH & Co. KG D-63755 Alzenau, Germany.

acetylacetonate precursors in a propionic solution with 0.25 M concentration which leads to films of 30 nm thick. They were grown in oxygen atmosphere at 900ºC for 8h. Further details of film growth of the YBCO layers as well as the CZO buffer layers can be found elsewhere [14-16]. The metallic ABAD tapes used in this work were also previously described [17].

Texture of the film was characterized by x-ray diffraction by using a general area detector diffractometer system (Bruker AXS GADDS). Critical current densities of the films were studied by performing angular resolved transport measurements up to 9 T in patterned films. Standard optical lithography was used to define tracks with typical widths in the range of 10-20 μm. Thickness of the YBCO films were determined by profilometer measurements of the studied tracks. In all the transport experiments, the current was applied parallel to the ab-planes (θ=90º) in the configuration of maximum Lorentz force between current and applied field.

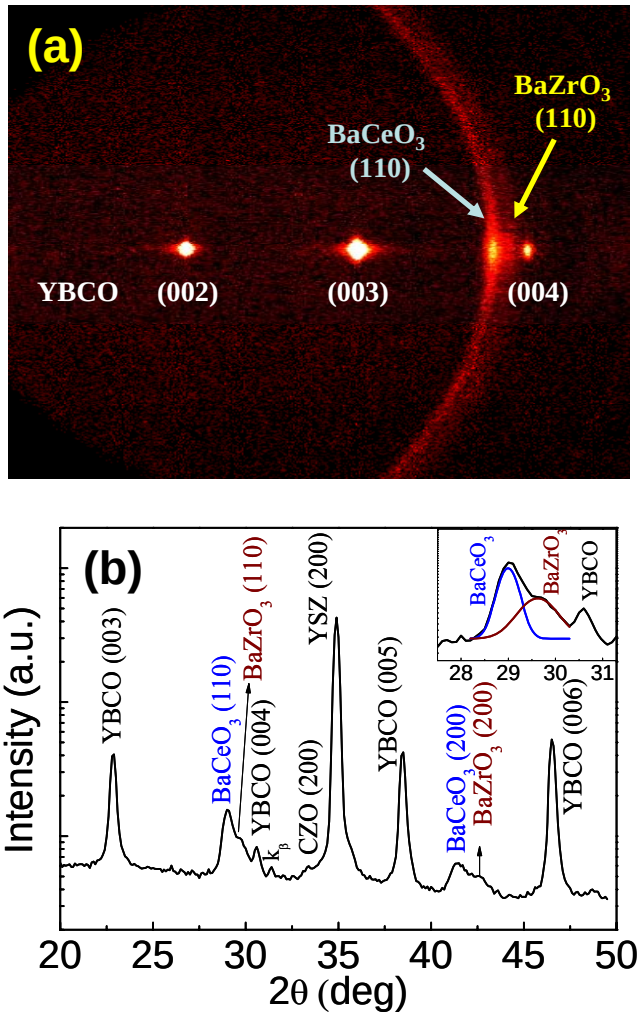

Fig. 1. (a) X-ray diffraction pattern obatained with a general area detector diffractometer system of a ^{TFA}YBCO-BZO nanocomposite film grown on ^{MOD}CZO/YSZ substrate. (b) Integration of the pattern in (a) along the χ angle. Now it can be observed the deconvolution of the peaks corresponding to $Ba(Ce,Zr)O_3$ and to the $BaZrO_3$ particles. The inset shows a detail around one of the peaks. The presence of significant signals of the (110) and (200) BZO reflections confirms the existence of two populations of nanoparticles: one epitaxial and the other one non-coherent with the YBCO matrix.

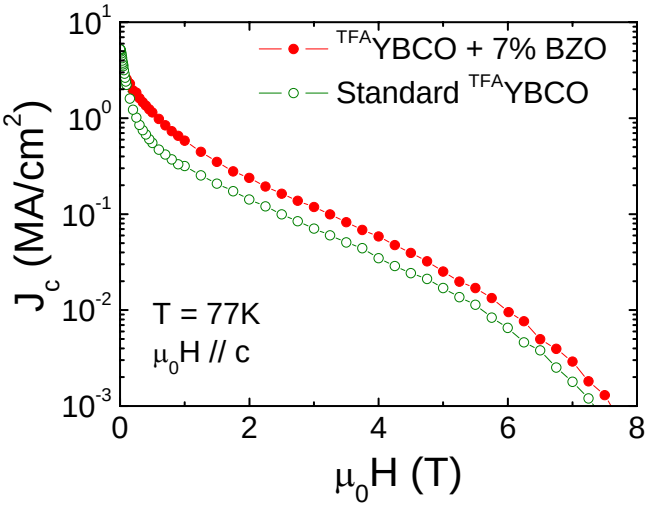

Fig. 2. Field dependence of the critical current density at 77K of a ^{TFA}YBCO-BZO nanocomposite (red solid circles) compared to the standard ^{TFA}YBCO film (open circles). Both films were grown on the same conditions on ^{MOD}CZO buffer layers on YSZ single crystals. Vortex pinning enhancement in the YBCO-BZO nanocomposite is evident.

III. RESULTS AND DISCUSSION

A typical x-ray diffraction pattern recorded using a general area detector system of an ^{TFA}YBCO-BZO nanocomopsite grown on ^{MOD}CZO/YSZ is shown in Fig. 1a. Epitaxial spots corresponding to the (00l) YBCO reflections can be easily identified. The absence of other reflections or rings in the YBCO phase excludes any non epitaxial fraction of the YBCO film. Usually in our standard ^{TFA}YBCO growth conditions, BZO particles can be formed [4]. For films grown on $LaAlO_3$ substrates, it was previously demonstrated that two populations of BZO nanoparticles coexist: i) epitaxial particles nucleating at the interface with the substrate and ii) non-coherent BZO particles randomly distributed in the YBCO matrix and mainly responsible of the enhanced pinning behavior observed in those nanocomposites [4, 8]. Thus, the identification of these random BZO particles is a crucial clue in the study of such nanocomposites. In the present case, however, the reactivity between YBCO and CZO, and the subsequent formation of $Ba(CeZr)O_3$, makes more difficult such identification by means of x-ray diffraction due to the similarity between their respective lattice parameters. In order to increase the signal-to-noise ratio we have performed an χ-integration of the pattern of Fig. 1a. The result of this integration is plotted as a θ-2θ graph in Fig. 1b. Now, in this figure we can observe that the discrimination between $BaZrO_3$ nanoparticles and $Ba(CeZr)O_3$ is possible (see the detail of the inset). Fig. 1b shows that both (110) polycrystalline reflection and (200) epitaxial reflection of BZO are present thus confirming the existence of both populations of BZO nanoparticles. Although more microstructural studies are underway to confirm these results, we can safely propose that the mechanisms of YBCO-BZO formation on CZO layers are similar to those on $LaAlO_3$ single crystalline substrates [4].

Let us now to turn our attention to the pinning properties of ^{TFA}YBCO-BZO nanocomposites grown on ^{MOD}CZO buffer layers. Figure 2a shows the magnetic field dependence

(parallel to the c-axis) of the critical current density J_c at 77K of an ^{TFA}YBCO-BZO film on ^{MOD}CZO/YSZ (solid red circles). We observe that, in spite of a reduction of the self-field critical current value, J_c=5.2MA/cm^2 for the standard ^{TFA}YBCO and J_c=3.1 MA/cm^2 for ^{TFA}YBCO-BZO, then in-field J_c of the nanocomposite largely exceeds that of the standard film (open circles), being already a factor two higher at 0.5T. In fact, the crossover roughly occurs when the low-field plateau of the standard film ends and J_c begins to fall following the typical power law decay. Thus, J_c(H) of the nanocomposite is much less field dependent indicating that the addition of BZO nanoparticles indeed enhance vortex pinning by introducing additional defects also in the conditions of YBCO growth on ^{MOD}CZO buffer layers.

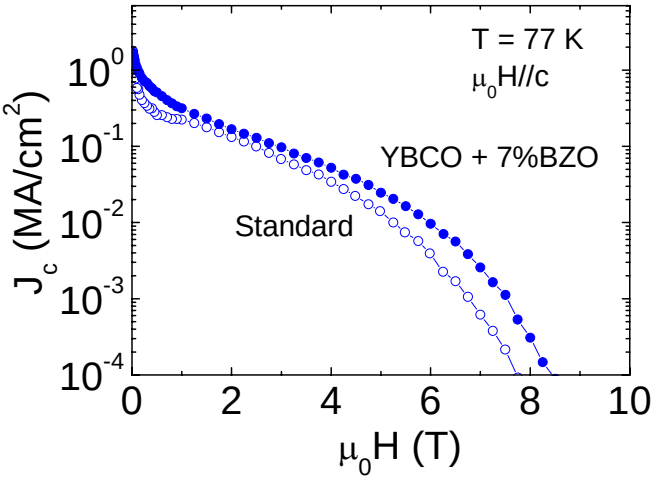

Fig. 3. Field dependence of the critical current density of a ^{TFA}YBCO-BZO nanocomposite coated conductor (solid circles) and of a standard ^{TFA}YBCO conductor (open circles). Both films are deposited on ^{MOD}CZO buffered ^{ABAD}YS/ SS tapes. Introduction of BZO nanoparticles strongly enhances vortex pinning for the whole regime of applied magnetic field studied.

These promising results invited us to the difficult task of growing ^{TFA}YBCO-BZO nanocomposites on MOD buffered metallic substrates. As said before, we have recently demonstrated that ^{TFA}YBCO coated conductors with promising values of J_c can be gown when deposited onto ^{MOD}CZO buffered ^{ABAD}YSZ/SS tapes [15]. This is a interesting medium cost approach that allows the study of all chemical architectures of film growth without the inherent difficulties of the extremely low cost approach of Ni- RABiT tapes. So, in Fig. 3 we present the magnetic field dependence of J_c parallel to the c-axis of an ^{TFA}YBCO-BZO tape (solid blue circles) compared to that of a standard ^{TFA}YBCO tape (open circles). The self-field value of J_c of the nanocomposite tape was J_c=1.7 MA/cm^2, similar to that of the standard tape. It is worthy to note that in both samples the full width at half maximum of the ϕ-scan around the (103) YBCO reflection was 5-6º. Thus both samples are of similar epitaxial quality and the different J_c(H) behavior can only be attributed to the modified vortex pinning in the nanocomposite and not to differences in the texture. It is clear that not only the absolute in-field J_c values of the nanocomposite are higher than that of the standard film but also the overall J_c(H) dependence is much smoother. This is also true even at low fields where critical current is dominated by the pinning of the grain boundaries [18, 19] and thus any enhancement of grain vortex pinning does not necessarily imply a higher J_c.

This granular behavior of the critical current of the tapes can be evidenced by comparing the J_c(H) of a ^{TFA}YBCO-BZO nanocomposite coated conductor with that of the ^{TFA}YBCO-BZO grown on single crystalline substrates, in both cases buffered with ^{MOD}CZO layers and grown in the very same conditions. An example of this comparison at 77K is shown in Fig. 4. Here we can observe the initial reduction at low fields of the absolute value of the critical current density originated by the presence of grain boundaries in the tape [18, 19]. At high fields and up to the irreversibility line, both critical currents are equal. This high field regime is dominated by the pinning of Abrikosov vortices in the superconducting grains and it reveals that grain pinning mechanisms of the nanocomposites in the tape and in the single crystal are identical.

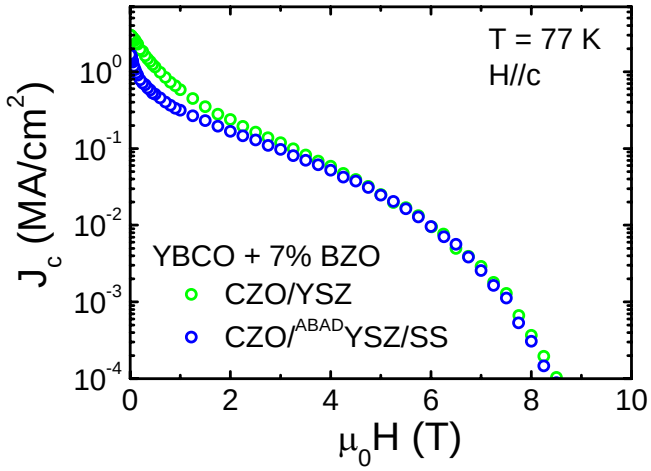

Fig. 5. Field dependence of the critical current density of two YBCO-BZO nanocomposites: one grown on YSZ single crystals (green circles) and the other grown on ^{ABAD}YSZ/SS tapes (blue circles). In both cases substrates were buffered with metallorganic deposited $(Ce,Zr)O_2$ buffer layers. At low fields J_c of the tape is dominated by grain boundary pinning while, at high fields, it is grain Abrikosov pinning that controls J_c and thus both values are equal.

An important point to note for some applications is that (at least at 77K) the magnetic field where the J_c of the nanocomposite tape achieves the value of the single crystals is found to be μ_0H = 4 T, much higher than the one observed in standard ^{TFA}YBCO tapes (μ_0H = 2 T). This is probably due to the smoother field dependence of J_c in ^{TFA}YBCO-BZO that enlarges the regime where grain boundary pinning dominates. These results should be taken into account when designing vortex pinning for certain field applications of coated conductors.

One of the most striking features of the enhanced vortex pinning properties in chemical solution deposited ^{TFA}YBCO-BZO nanocomposites is their angular behavior. Indeed, BZO particles induce a highly defective YBCO matrix that it is able to efficiently pin the vortices in the whole angular range and

for any magnetic field orientation. This isotropic effect has, as an interesting consequence, the strong reduction of the effective electronic anisotropy in the ^{TFA}YBCO-BZO films [4, 8], recently also observed in other doped YBCO samples [20]. For this, it is of the greatest importance to investigate the angular dependence of the critical current in the YBCO-BZO tapes presented here. This is done in Fig. 5 where we plot the $J_c(\theta)$ of the ^{TFA}YBCO-BZO tape (solid circles) at μ_0H=1T and 77K in comparison with an ^{TFA}YBCO standard tape (open circles). It can be seen that, as expected, the anisotropy in J_c is strongly reduced in the nanocomposite. Also, the overall J_c (θ) behaves clearly different and the peak in J_c when H//c (θ=180º) observed in the standard tape has been hidden in the nanocomposite. This peak is usually attributed to the presence of defects along the c-axis direction [21, 22] and its apparently absence in the nanocomposite implies that pinning is dominated by the isotropic contribution induced by the BZO inclusions [4, 8]. Although the physical origin of this reduced anisotropy needs to be elucidated it is clear that it is related to the modified microstructure of the YBCO matrix due to the introduction of nanoparticles [8]. Similar results have been reported in other chemical solution deposited nanocomposites [20].

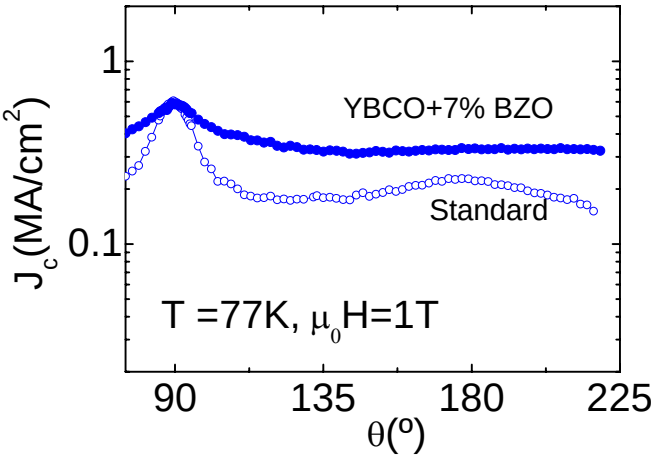

Fig. 4. Angular dependence at 77K and μ_0H=1T of the critical current density of a ^{TFA}YBCO-BZO nanocomposite (solid circles) and of a ^{TFA}YBCO standard coated conductor. Both samples were grown on ^{MOD}CZO/^{ABAD}YSZ/SS tapes. The reduced anisotropy of J_c in the nanocomposite is associated to the enhanced pinning due to the BZO nanoparticles.

IV. CONCLUSIONS

We have demonstrated that YBCO-BZO nanocomposites can be successfully grown by the trifluoroacetates route on ^{MOD}CZO buffered substrates, either YSZ single crystals or ABADYSZ/SS metallic tapes. In all the cases a clear improvement of vortex pinning capabilities was observed, with higher in field-J_c values and smoother magnetic field dependences of the critical current densities. The overall behavior of the ^{TFA}YBCO-BZO coated conductors is thus very similar to the same nanocomposite grown on $LaAlO_3$ single crystals previously reported [4, 8], i.e., a strong isotropic vortex pinning enhancement due to the highly defective YBCO matrix induced by the randomly oriented BZO nanoparticles. The present results show that this approach can be successfully used in the fabrication of coated conductors with improved in-field performances.

REFERENCES

[1] J. L. Macmanus-Driscoll *et al.*, "Strongly enhanced current densities in superconducting coated conductors of $YBa_2Cu_3O_7$+$BaZrO_3$ " *Nat. Mater.*, vol. 3, pp. 439-443, 2004.

[2] T. Haugan, P. N. Barnes, R. Wheeler, F. Meisenkothen, and M. Sumption, "Addition of nanoparticle dispersions to enhance flux pinning of the $YBa_2Cu_3O_{7-x}$ superconductor," *Nature,* vol. 430, pp. 867-870, 2004.

[3] S. Kang *et al.*, "High-performance high-T-c superconducting wires," *Science,* vol. 311, pp. 1911-1914, 2006.

[4] J. Gutiérrez *et al.*, "Strong isotropic flux pinning in solution-derived $YBa_2Cu_3O_{7-x}$ nanocomposite superconductor films," *Nat. Mater.,* vol. 6, pp. 367-373, 2007.

[5] S. R. Foltyn *et al.*, "Materials science challenges for high-temperature superconducting wire," *Nat. Mater.,* vol. 6, pp. 631-642, 2007.

[6] Y. Yamada *et al.*, "Epitaxial nanostructure and defects effective for pinning in (Y,Re)$Ba_2Cu_3O_{7-x}$ coated conductors," *Appl.Phys.Lett.,* vol. 87, p. 132502, 2005.

[7] A. Pomar *et al.*, "Tuning the superconducting properties of $YBa_2Cu_3O_7$ tapes grown by chemical methods," *Physica C,* vol. 460, pp. 1401-1404, 2007.

[8] T. Puig *et al.*, "Vortex pinning in chemical solution nanostructured YBCO films," *Supercond. Sci. Technol.,* vol. 21, p. 034008, 2008.

[9] N. M. Strickland *et al.*, "Enhanced flux pinning by $BaZrO_3$ nanoparticles in metal-organic deposited YBCO second-generation HTS wire," *Physica C,* vol. 468, pp. 183-189, 2008.

[10] S. Engel *et al.*, "Enhanced flux pinning in $YBa_2Cu_3O_7$ layers by the formation of nanosized $BaHfO_3$ precipitates using the chemical deposition method," *Appl.Phys.Lett.,* vol. 90, p. 102505, 2007.

[11] D. M. Feldmann *et al.*, "Influence of growth temperature on critical current and magnetic flux pinning structures in $YBa_2Cu_3O_{7-x}$," *Appl.Phys.Lett.,* vol. 91, p. 162501, 2007.

[12] N. Roma *et al.*, "Acid anhydrides: a simple route to highly pure organometallic solutions for superconducting films," *Supercond. Sci. Technol.,* vol. 19, pp. 521-527, 2006.

[13] K. Zalamova *et al.*, "Smooth stress relief of trifluoroacetate metal-organic solutions for $YBa_2Cu_3O_7$ film growth," *Chem. Mat.,* vol. 18, pp. 5897-5906, 2006.

[14] M. Coll *et al.*, "All chemical $YBa_2Cu_3O_7$ superconducting multilayers: critical role of CeO_2 cap layer flatness," Submitted to J Mater Res.

[15] V. R. Vlad *et al.*, "Growth of chemical solution deposited ^{TFA}YBCO/^{MOD}(Ce,Zr)O_2/^{ABAD}YSZ/SS coated conductors," *This conference*.

[16] M. Coll *et al.*, "Nanostructural control in solution derived epitaxial $Ce_{1-x}Gd_xO_{2-y}$ films," *Nanotechnology,* vol. 19, p. 395601, 2008.

[17] A. Usoskin *et al.*, "Processing of long-length YBCO coated conductors based on stainless steel tapes," *IEEE Trans. Appl. Supercond.,* vol. 17, pp. 3235-3238, 2007.

[18] L. Fernandez *et al.*, "Influence of the grain boundary network on the critical current of $YBa_2Cu_3O_7$ films grown on biaxially textured metallic substrates," *Phys. Rev. B,* vol. 67, p. 052503 2003.

[19] A. Palau, T. Puig, J. Gutierrez, X. Obradors, and F. de la Cruz, "Pinning regimes of grain boundary vortices in $YBa_2Cu_3O_{7-x}$ coated conductors," *Phys. Rev. B,* vol. 73, p. 132508, 2006.

[20] Z. Chen *et al.*, "Three-dimensional vortex pinning by nano-precipitates in a Sm-doped $YBa_2Cu_3O_{7-x}$ coated conductor," *Supercond. Sci. Technol.,* vol. 20, pp. S205-S210, 2007.

[21] A. Diaz, L. Mechin, P. Berghuis, and J. E. Evetts, "Evidence for vortex pinning by dislocations in $YBa_2Cu_3O_{7-delta}$ low-angle grain boundaries," *Phys. Rev. Lett.,* vol. 80, pp. 3855-3858, 1998.

[22] L. Civale *et al.*, "Angular-dependent vortex pinning mechanisms in $YBa_2Cu_3O_7$ coated conductors and thin films," *Appl.Phys.Lett.,* vol. 84, pp. 2121-2123, 2004.